1 **Title:** Rapid fluctuations in histamine associated with intake of

2 nutritive and non-nutritive solutions

3

4 **Authors:** Volcko KL[1], Gresch A[2], Benowitz B[3], Taghipourbibalan H[1], Visser M[1], Stuber GD[3],

5 Gordon-Fennell AG[3], Patriarchi T[2,4], McCutcheon JE[1]

6

7 **Affiliations:**

8 1 Department of Psychology, UiT The Arctic University of Norway, 9019 Tromsø, Norway

9 2 Institute of Pharmacology and Toxicology, University of Zürich, 8006 Zürich, Switzerland

10 3 Center for the Neurobiology of Addiction, Pain, and Emotion, Department of Anesthesiology

11 and Pain Medicine, Department of Pharmacology, University of Washington, 98195 Seattle, USA

12 4 Neuroscience Center Zurich, University and ETH Zürich, 8006 Zürich, Switzerland

13

14 **Corresponding authors:**

15 James E. McCutcheon

16 Email: j.mccutcheon@uit.no

17 Phone: +47 776 44 593

18 Address: Department of Psychology, UiT The Arctic University of Norway, 9019 Tromsø, Norway

19

20 Tommaso Patriarchi

21 Email: patriarchi@pharma.uzh.ch

22 Phone: +41 044-635-5921

23 Address: Winterthurerstrasse 190, Building Y17, room J22, CH-805, Zürich, Switzerland

24

25

26 **Abbreviations:**

27 Paraventricular nucleus of the hypothalamus (PVH)

28 Ventromedial hypothalamus (VMH)

29 H1 receptor (H1R)

30

Abstract

The neurotransmitter histamine is involved in control of food intake, yet its dynamics during individual feeding episodes remain unexplored. Therefore, we used the novel genetically-encoded histamine sensor, HisLightG, combined with fiber photometry to measure histamine release in two hypothalamic regions critical for the food-suppressive effects of histamine, the paraventricular nucleus of the hypothalamus (PVH), and the ventromedial hypothalamus (VMH). Male mice were tested under different conditions to assess whether hunger, time of day, or the caloric content of the solution they were given affected histamine fluctuations. We found that histamine levels changed rapidly in response to eating. These histamine fluctuations were influenced by experimental conditions, with slightly smaller responses when the test solution was sucralose (both regions) or during the light cycle (PVH only). Notable regional differences were identified, such that in the PVH histamine rebounded to baseline levels, whereas in the VMH histamine remained lower than baseline for at least 10 seconds after licking ceased. In a separate cohort of male and female mice, enhancing histamine tone via administration of a histamine precursor (L-histidine) reduced the number of licks across multiple sucrose concentrations. Together, these findings indicate that histaminergic activity is modulated rapidly during ingestive episodes, and that understanding these release patterns will give insight into histamine's role in appetite suppression.

2

1. Introduction

The mechanisms that govern meal termination and reductions in food intake are complex and intertwined. The neurotransmitter and neuromodulator histamine plays an important role in ingestive behavior and many well-known satiety signals, including leptin (Morimoto et al., 1999; Toftegaard et al., 2003), amylin (Lutz et al., 1996; Mollet et al., 2003), cholecystokinin (Attoub et al., 2001), and glucagon-like peptide-1 (Gotoh et al., 2005), require histamine in order to exert their effects on eating behavior. Histamine may be responding directly to some of these signals – for example, amylin fibers and histaminergic neurons are found in close proximity (D'Este et al., 2001) – but there is likely also indirect input, such as through the melanocortin system (Michael et al., 2020) or noradrenaline (Kurose & Terashima, 1999).

Histamine is involved in many physiological processes besides eating, and can either stimulate or suppress food intake depending on the precise location and receptor subtype activated. The bulk of previous research measuring histamine levels in the brain used microdialysis, a technique which is limited by a relatively large sampling area (e.g., "anterior hypothalamus") as well as low temporal resolution (e.g. 20-30 min between samples). Fast-scan cyclic voltammetry has also been used to measure histamine with high temporal resolution *in vivo* (Berger et al., 2022; Samaranayake et al., 2015). However, properties of the molecule and its release patterns make these studies difficult to perform and have limited utility for studying spontaneous histamine release during naturally occurring behaviors (i.e., outside of stimulation of histamine containing fibers). Recent advances in genetically-encoded fluorescent neurotransmitter sensors have allowed *in vivo* neurotransmitter release to be combined with fiber photometry yielding measurements with high chemical, temporal and spatial precision (Patriarchi et al., 2019; Simpson et al., 2024). So far, a histamine sensor, GRAB-HA, has been used in two other studies showing fluctuations during sleep-wakefulness (Dong et al., 2023) and after an aversive stimulus (Lin et al., 2023). To our knowledge, however, no one has previously recorded histamine fluctuations using fiber photometry during eating behavior. Moreover, unlike the other studies cited, we use the novel histamine sensor HisLightG (Kagiampaki et al., 2023).

Central histamine-producing neurons are located in the tuberomammillary nucleus in the posterior hypothalamus (Panula et al., 1984; Watanabe et al., 1984), and project widely throughout the brain, including many hypothalamic nuclei (Lin et al., 2023; Panula et al., 1989). Histamine acts on several receptor subtypes, although it is the H1 receptor (H1R) that mediates suppressive effects of histamine on food intake (Fukagawa et al., 1989; Kurose & Terashima, 1999; Lecklin et al., 1998; Masaki et al., 2004; Morimoto et al., 1999; Ookuma et al., 1989; Sakata et al., 1988). H1Rs are expressed in many parts of the brain, with a high density found in

3

83   both the ventromedial hypothalamus (VHM) and the paraventricular nucleus of the

84   hypothalamus (PVH) (Futagawa et al., 2024). Infusions of H1R antagonists, or drugs to inhibit

85   local histamine production, into specific hypothalamic nuclei have indicated that these two

86   regions – the VMH and the PVH – are the critical sites of action for histamine to attenuate eating

87   (Ookuma et al., 1989, 1993; Sakata et al., 1988, 1990, 1991).

88   We wanted to examine the patterns of histamine release in the PVH and the VMH during

89   eating bouts in mice, using fiber photometry and the new histamine sensor, HisLightG

90   (Kagiampaki et al., 2023). Histamine levels in the hypothalamus are sensitive to time of day (Doi

91   et al., 1994; Mochizuki et al., 1992; Sakata et al., 1988). We therefore recorded histamine

92   fluctuations during both the dark and light phase. Additionally, histamine levels may or may not

93   be influenced by hunger status (Itoh et al., 1991; Sakata et al., 1994). Consequently, we

94   measured histamine in both *ad libitum* and food restricted conditions. Finally, in a separate

95   experiment to determine how histamine levels shape consumption over a range of rewarding

96   solutions, we manipulated histamine levels by providing the precursor, L-histidine, and measured

97   licking for different concentrations of sucrose.

98   **2. Methods**

99   *2.1 In vitro experiments*

100 *2.1.1 Cell culture, confocal imaging and quantification*

101   HEK293T cells (ATCC #CRL-3216) were cultured in DMEM medium (Thermo Fisher)

102 supplemented with 10% FBS (Thermo Fisher) and 100 µg/ml Penicillin-Streptomycin mix

103 (Thermo Fisher) and incubated at 37°C with 5% CO_2. Cells were transfected at 50-60%

104 confluency in glass-bottomed dishes using PolyFect Transfection Reagent (Qiagen) according to

105 manufacturer instructions, and used for follow-up experiments 24–48 h after transfection.

106 Before imaging, cells were rinsed with 1 mL of Hank's Balanced Salt Solution (HBSS, Life

107 Technologies) containing $CaCl_2$ and $MgCl_2$ supplemented with 30 mM HEPES, both from

108 Thermo Fisher. All cells were imaged at room temperature in glass bottom dishes using HBSS

109 with 30 mM HEPES. Imaging was performed using Zen Blue software on an inverted Zeiss LSM

110 800 confocal microscope equipped with 488 nm laser and a 40X oil-based objective. During

111 timelapse imaging, ligands were applied manually using a micropipette to reach a final

112 concentration of 10 µM. For quantification of the fluorescence response $\Delta F/F_0$, regions of

113 interest (ROI) enclosing isolated cell membranes were selected manually using the threshold

114 function of Fiji (ImageJ). Sensor response ($\Delta F/F_0$) was calculated as follows: $(F(t) - F_0)/F_0$ with

115   F(t) being the ROI mean gray value at each time point (t), and F_0 being the mean gray value of

116   the ten timepoints immediately prior to ligand addition.

117   *2.2 Photometry Experiments*

118   *2.2.1 Animals*

119   Adult male C57BL/6NRj mice (6 – 8 weeks old) were purchased from Janvier (France)

120   and housed in a temperature- and humidity-controlled room, maintained on a 12:12 light:dark

121   cycle (lights-on at 00:00). Two mice shared each cage, separated by a perforated divider that

122   allowed visual, olfactory, and auditory communication but prevented major physical contact.

123   Water and food were available *ad libitum* unless mice were undergoing food restriction. All

124   animal care and experimentation followed the EU directive 2010/63/EU for animal experiments,

125   and was approved by the National Animal Research Authority in Norway.

126   *2.2.2 Surgical procedures*

127   Surgery was performed after a minimum of 5 days of habituation to the animal facility.

128   Mice (n = 23) were anesthetized with isoflurane and secured in a stereotaxic apparatus (Kopf,

129   Tujunga, CA, USA). Each mouse was given subcutaneous injections of buprenorphine (0.1

130   mg/kg; Temgesic) and meloxicam (5 mg/kg; Metacam) to provide systemic analgesia, as well as

131   bupivacaine (1 mg/kg; Marcain) as a local anesthetic. A small burr hole was made above the

132   target area (see Table 1 for coordinates; all coordinates based on a flat skull) and 500 nl (0.6 x

133   10^9 vg) of AAV-9/2-hSyn1-chI-HisLightG-WPRE-bGHp(A) (#10264; ETH Viral Vector Facility)

134   was infused at a rate of 100 nl / minute using a Nanofil syringe with 33 g blunt needle and UMP3

135   microsyringe pump (WPI; Sarasota, FL, USA). The needle remained in place for 10 min to allow

136   the virus to diffuse. Next, a fiber optic cannula (1.25 mm ceramic ferrule, 0.4 NA, 400 µm core;

137   RWD) was lowered slowly to just above the virus injection. The fiber optic was secured to the

138   skull with dental cement (Superbond C&B). Each mouse received meloxicam 2 days

139   postoperatively.

140   *Table 1: surgical coordinates*

Target	Medial-Lateral	Anterior-Posterior	Dorsal-Ventral (virus)	Dorsal-Ventral (fiber)
Paraventricular nucleus of the hypothalamus	0.3 mm lateral to midline	0.8 mm posterior to bregma	4.70 mm ventral to skull	4.60 mm ventral to skull
Ventromedial nucleus	0.3 mm	1.20 mm	5.65 mm ventral	5.55 mm ventral

of the hypothalamus	lateral to midline	posterior to bregma	to skull	to skull

2.2.3 Testing apparatus

Testing took place in operant chambers (24 cm x 20 cm; Med Associates, Fairfax, VT). The fan was on continuously during testing. When mice were tested during their dark phase, the house light was off in the testing chambers, and when the mice were tested during their light phase, the house light was on in the operant chambers. Solutions were delivered through blunted 18 g needles attached to 5 ml syringes via flexible tubing. These syringes were mounted on syringe pumps that dispensed the solution when licks were detected via a contact lickometer. These pumps were controlled by MEDPC-V software (Med Associates).

While the mice freely explored the operant chambers and licked solutions, histamine activity was recorded via fiber photometry. An RZ10x system and Synapse software (Tucker-Davis Technologies, Alachua, FL, USA) controlled two LED light sources, one blue (465 nm) and one violet (405 nm). The blue light was sinusoidally modulated at 330 Hz and the violet at 210 Hz. A fluorescence minicube (Doric Lenses, Quebec, Canada) combined the blue and violet wavelengths. A 400 µm optical patch cord (Doric Lenses) transmitted the light to the mouse, where the cable and ferrule were attached by a black ceramic sleeve (RWD). This same cable was used to collect light emitted from the brains of the mice. This light was detected by a femtowatt photoreceiver (#2151; Newport, Irvine, CA, USA).

2.2.4 Testing procedures

Each mouse underwent a series of testing sessions in different blocks, with each block a different condition. The order of the blocks was the same for all mice. Testing began at least 12 days after surgery and after mice had been habituated to having a cable attached to their fiber optic implant. The four blocks were 1) *ad libitum* light, 2) food restricted dark, 3) *ad libitum* dark, and 4) *ad libitum* sucralose. In the *ad libitum* light block ("Light"), mice with *ad libitum* food and water were tested during the light phase. They were placed in operant chambers for three 30-minute sessions on different days, in which 1 kcal / ml "Ensure" (Nestle Resource Complete neutral flavor) was continuously available through a spout. In the food restricted dark block ("Restricted"), mice were tested in the dark while food restricted. Food restriction was achieved by giving 2.5 – 3 g of chow to each mouse each day; this resulted in approximately 5-10 % weight loss. In this phase they were again given "Ensure" during three 30 min sessions. The *ad libitum* dark block ("Dark") was identical to the Light block except mice were tested during their dark phase and only tested in 2 sessions. Lastly, in the *ad libitum* sucralose block ("Sucralose")

172 mice were tested without food restriction in the dark, but given 2 mM sucralose in the single 30
173 min session.

2.2.5 Histology

175   Only mice with virus and fibers placed correctly were included in the final analysis. To
176 check placements, brains were collected at the end of the experiment. Briefly, mice were deeply
177 anesthetized with 0.3 ml of ZRF mix (zolazepam, 3.3 mg/ml; tiletamine, 3.3 mg/ml; xylazine, 0.45
178 mg/ml; fentanyl, 2.6 ug/ml). The mice were then transcardially perfused with heparinized saline
179 and 4% paraformaldehyde. Brains were removed, postfixed overnight in 4% paraformaldehyde,
180 and placed in 30% sucrose with Proclin. A microtome (Leica, Deer Park, IL; USA) was used to
181 cut brains into 40 µm coronal sections. Every third section was directly mounted onto a
182 Superfrost Plus slide and coverslipped. The native fluorescence of the viral injections was used
183 to determine the location and spread of the injection, and the fiber tract used to assess location
184 of the implant.

2.3 Histamine manipulation experiments
2.3.1 Animals

187   Adult male and female C57BL/6J mice (n=4 of each sex) were bred and housed in the
188 animal facility at University of Washington. Mice were kept on reverse 12h light:dark cycle
189 (lights-on at 21:00) and behavioral experiments were conducted within the dark cycle. Mice
190 were single-housed to prevent damage to the head fixation device, provided with water *ad*
191 *libitum*, and during experiments were food restricted to ~90% of free-feeding weight by providing
192 a ration of food (2.5-4 g / day) depending on weight change from the previous day. All animal
193 procedures were pre-approved by the Institutional Animal Care and Use Committee (IACUC) at
194 University of Washington (protocol 4450-01).

2.3.2 Surgery

196   Mice (n=8) were anesthetized with isoflurane (5% for induction, 1.5 – 2% for
197 maintenance), injected with analgesic (carprofen, 10 mg/kg, s.c.), and the scalp was shaved
198 using electric clippers. Mice were mounted in a stereotaxic frame with heat support and the
199 scalp was injected with local anesthetic (lidocaine, 2%, s.c.) and sterilized using ethanol and
200 betadine. An incision was made using a scalpel and the skull was cleared of tissue and scored
201 with the pointed end of the scalpel. The skull was leveled and 2 micro screws were inserted into
202 burr holes drilled in the lateral portion of the occipital bone, with one additional screw placed in

7

203   the rostral portion of the skull. A head fixation device (a head plate; 0.8 mm stainless steel 304

204   series, sendcutsend.com) was attached the skull and screws using Super Glue and then dental

205   cement was used to encase a portion of the head bar and the screws. Once fully set, mice were

206   removed from the stereotaxic frame, allowed to recover with heat support, and then returned to

207   their home cage and allowed to recover for at least 1 week before food restriction began.

208   *2.3.3 Behavior in multispout apparatus*

209   Habituation and training took place as described in (Gordon-Fennell et al., 2023). Briefly,

210   mice were first habituated to gentle scruffing, handling by their head bar, and light restraint within

211   a 50 mL conical over 3 days. Next, mice were given free access to sucrose when head-fixed in

212   the multispout apparatus for 10 min on a single day. Mice were then trained on the multispout

213   apparatus with multiple concentrations of sucrose available. The assay consisted of daily

214   sessions with 100 trials with 3 s access to one of five different sucrose concentrations (0%

215   (water), 5%, 10%, 20%, and 30%, 20 trials of each). Solutions were presented pseudorandomly

216   with an inter-trial interval of 12.5 ± 2.5 s. Licks were detected using a capacitive touch sensor

217   (Adafruit MPR121). Once mice had reached stable behavior in which lick rate showed a

218   monotonic relationship with sucrose concentration, the pharmacological manipulation began. In

219   2 consecutive sessions mice received either L-histidine (500 mg/kg) or vehicle (saline) i.p. 2 h

220   before being tested in the multispout apparatus. Order of administration was counterbalanced

221   across mice and sexes.

222   *2.4 Experimental Design and Statistical Analysis*

223   *2.4.1 In vitro experiments*

224   *In vitro* experiments used Welch ANOVA with Dunnett's multiple comparison test. Each

225   neurotransmitter was tested on 30 cells. All experiments were repeated 3 times with similar

226   results. A p-value of < 0.05 was considered significant.

227   *2.4.2 Photometry experiments*

228   For the photometry experiment, all statistical analyses were conducted using JASP

229   (https://jasp-stats.org/). Post hoc tests were Holm corrected for multiple comparisons. Data from

230   mice in the PVH cohort and the VMH cohort were analyzed separately, except for when they

231   were directly compared and when they were combined. TDT files included timestamps of licks

232   relayed to the TDT system through MED-PC and its lickometer, as well as the photometry

233   streams for HisLightG and the 405 nm isosbestic control. Raw data files are available at the

234   following link: http://doi.org/10.5281/zenodo.13981427. Data were extracted using custom

235   Python scripts available at https://github.com/mccutcheonlab/hislightg. The photometry signal

236   was corrected for bleaching and artefacts by using FFT-based correction method to subtract the

237   405 nm signal from the 465 nm signal, as previously described (Konanur et al., 2020).

238   Several aspects of licking behavior were analyzed: average licks per session, average

239   number of bouts per session, and average length of bouts per session. Lick bouts were defined

240   as a cluster of 3 or more licks with at least 10 seconds separating one bout from another.

241   Repeated measures ANOVA with Condition (Restricted, Light, Dark, and Sucralose) as within-

242   subjects factor were conducted for each of these parameters. We did not expect mice with PVH

243   or VMH placements to differ in behavior. This was confirmed in a preliminary analysis finding no

244   main effect of Region in licks, number of lick bouts, or length of lick bouts. We therefore

245   combined mice from both regions for subsequent analyses.

246   Peri-event traces (hereafter, "snips") of the photometry trace corresponding to the 5 s

247   before a lick bout, and lasting 10 seconds after licking ended were created for each lick bout for

248   each mouse. Of the total lick bouts, we created snips for those lasting at least 8 seconds (in the

249   Restricted analysis of PVH vs VMH), or 4 seconds (for the analysis between conditions, due to

250   the low number of longer lick bouts in the Sucralose condition). Artifacts were removed by

251   comparing the absolute difference between consecutive time points and if this was greater than

252   a threshold of 12, that lick bout was discarded. To account for different durations of each bout,

253   only the first 6 s and last 2 s of licking were included. Snips were normalized by z-scoring, using

254   the 5 s before licking as baseline; a baseline was calculated for each snip.

255   We used a strategy similar to that described in (Jean-Richard-dit-Bressel et al., 2020) to

256   conduct waveform analyses of histamine fluctuations. First, we created a bootstrapped estimate

257   of the mean using all lick bouts from a given region and condition, sampling 1000 times with

258   replacement. A 95% confidence interval was then constructed around the mean. We set a

259   consecutive threshold of 6 bins (equivalent to 0.6 s), corresponding to the low-pass filter of the

260   photometry signal. As such, if the confidence interval did not include zero for at least 6

261   consecutive time bins, the period was determined as a true fluctuation in histamine. Similarly, for

262   a comparison between PVH and VMH in the restricted condition, we compared the confidence

263   intervals for the PVH and VMH and when they were not overlapping for at least 6 consecutive

264   time bins, we considered them different from each other.

265   *2.4.3 Multispout experiments*

9

266   For the multispout experiments, we analyzed the data with a repeated-measures ANOVA
267   with sucrose concentration as within-subjects factor and injection (vehicle or L-histidine) as
268   between-subjects factor. We also performed planned comparisons between injections at each
269   sucrose concentration to test the hypothesis that at each concentration, mice with L-histidine
270   injections would lick less than mice with vehicle injections.

271   **3. Results**

272   *3.1 In vitro results*

273   The fluorescent sensor HisLightG was created by combining the human H4 histamine
274   receptor with a portion of the fluorescent sensor for dopamine, dLight1.3b (Fig 1A; Kagiampaki
275   et al., 2023). To confirm specificity of HisLightG to histamine, we performed *in vitro* tests in which
276   HEK293T cells were transfected and the fluorescent response to a variety of neurotransmitters
277   was measured. Relative to control (Hank's Buffered Saline Solution), addition of 10 µM
278   histamine caused an approximate 150% increase in sensor fluorescence (Fig 1B; $p < 0.001$).
279   Application of acetylcholine also led to a significant increase in fluorescence ($p < 0.001$)
280   although this response was only a 12% increase, approximately 13 times smaller than the
281   response to histamine, and so is unlikely to substantially contaminate fluorescent signals
282   measured *in vivo*. All other neurotransmitters tested were without effect (Fig 1C; all p's > 0.05).

283   *3.2 Photometry results*
284   *3.2.1 Licking behavior across time of day, hunger state, and caloric content*

285   Licking behavior in the different conditions – Restricted, Light, Dark, and Sucralose – was
286   compared across all mice that were included in the photometry analysis, without regard to
287   whether the PVH or VMH was targeted. The schematic in Fig 2A details how hunger state, time
288   of day, and nutritional value of the solution were manipulated in each of these four conditions.
289   We plotted total lick bouts of any length (the number of bouts that included at least 3 licks which
290   were separated by another licking bout by at least 10 seconds, with no criteria for length in time
291   of the lick bouts) in all sessions against bout length, for each of the conditions (Fig 2B) as well as
292   lick frequency for each condition (Fig 2C). Next, we divided these data by session and
293   statistically examined average licks per session, average number of lick bouts per session, and
294   average length of lick bouts per session.

295   The average number of licks per 30 min session (Fig 2D) had a significant main effect of
296   Condition ($F_{3, 39} = 98.604$, $p < 0.001$). Post hoc tests revealed that each condition had different

297 average numbers of licks per session. The average number of total bouts per session (Fig 2E)
298 also differed by Condition ($F_{3, 39} = 17.149$, p <0.001). Post hoc tests showed that the number of
299 bouts was equivalent in the Restricted and Sucralose conditions, which both had more bouts
300 than the Light and Dark conditions. Dark had more bouts than Light did. Average length of lick
301 bouts in seconds (Fig 2F) had a significant main effect of Condition ($F_{3, 39} = 29.709$, p <0.001).
302 Post hoc tests showed that lick bouts were shorter in the Sucralose condition than any of the
303 others.

304 Thus, by manipulating three variables - hunger state, time of day, and nutritional value of
305 the solution - we created multiple different food intake scenarios that we could analyze to see
306 whether each factor affected measured histamine release.

307 *3.2.2 Expression of HisLightG in the PVH and in the VMH*

308 We examined viral spread and fiber placement in brains from mice in the PVH cohort
309 (n=11) and the VMH cohort (n=12). In the PVH cohort 4 mice were excluded due to not having
310 viral expression in the PVH, and in the VMH cohort 2 mice were excluded for poor virus
311 expression and 3 for improper fiber location. This left a total of 7 mice for each region; all
312 subsequent analyses were restricted to mice with viral expression in, and fiber tip near, the PVH
313 (Fig 3A and Fig 3C) or VMH (Fig 3B and Fig 3D).

314 *3.2.3 Changes in histamine associated with lick bouts, in the PVH and VMH*

315 Our primary interest was in examining how histamine may fluctuate during and around
316 consumption. As seen above, the most lick bouts occurred during the Restricted condition, so we
317 looked closely at mice in this condition expressing HisLightG in the PVH and in the VMH.
318 The z-scored change in fluorescence associated with lick bouts showed a similar pattern across
319 lick bouts and sessions in both the representative PVH mouse (Fig 3E) and VMH mouse (Fig
320 3F), and it appeared that there were some differences between the regions, especially after the
321 end of the lick bout.

322 To analyze these changes, we performed waveform analysis on histamine fluctuations in
323 the PVH and VMH during the Restricted condition (Jean-Richard-dit-Bressel et al., 2020). A total
324 of 248 lick bouts (each of the 7 mice contributing between 18-45 bouts) from the PVH and 238
325 lick bouts (each of the 7 mice contributing between 19-43 bouts) from the VMH were included
326 (Fig 4A). These lick bouts were used to construct a bootstrapped mean and 95% confidence
327 interval for each region. In the PVH, histamine was reduced below zero 1.5 s after licking
328 started, and remained below zero for 2.8 s after licking stopped. Between 4.4 s and 10 s after

11

329 licking stopped, histamine in the PVH rebounded to above zero. In the VMH, however, histamine

330 fell below zero 0.2 s after licking started and remained suppressed throughout the lick bout and

331 for at least 10 s after licking ceased. Comparing the confidence intervals for the histamine signal

332 in the PVH and in the VMH revealed a significant difference (i.e., no overlap between the two

333 regions) in the last 2 s of licking and throughout the 10 s of post-licking examined; during this

334 time, histamine was lower in the VMH than in the PVH (Fig 4B).

335 In addition to the waveform analysis, we conducted a more traditional area-under-the-

336 curve (AUC) analysis with epochs that we designated based on the behavior (i.e., the beginning

337 and end of a lick bout, and the 10 s following a lick bout divided into two equal 5s bins). Overall,

338 the conclusions drawn from the AUC analysis were aligned with those from with the waveform

339 analysis (Supplemental Figure 1).

340

341 *3.2.3 Changes in histamine across time of day, hunger state, and caloric content*

342 To see if histamine was sensitive to time of day, hunger state, or the caloric content of the

343 solution, we compared the histaminergic response between conditions in the PVH (Fig 5A) and

344 in the VMH (Fig 5B). Total lick bouts included in this analysis and the number of bouts from each

345 mouse can be found in Table 2. In the PVH, we saw little difference in histamine in the Restricted

346 and Dark conditions. In the Light and Sucralose condition, histamine took longer to rebound to

347 above zero after licking stopped. In the VMH, histamine was suppressed to below zero in the

348 Restricted, Dark, and Light conditions within a second of licking and remaining low for the full 10

349 s after licking stopped; in the Sucralose condition histamine did not fall below zero until the last 2

350 s of the lick bout.

351

352 *Table 2: Number of lick bouts contributing to the photometry analysis*

Region	Condition	Total lick bouts	Bouts per mouse
PVH	Restricted	248	18-54
	Dark	107	5-23
	Light	104	9-22
	Sucralose	85	4-22
VMH	Restricted	270	19-54
	Dark	126	10-23
	Light	77	2-22
	Sucralose	74	8-16

353

3.3 Behavioral manipulation of histamine levels

355   We examined licking behavior to different concentrations of sucrose in the OHRBETS
356   multispout in mice given injections of the histamine precursor, L-histidine, or vehicle (Fig 6A).
357   Raster plots with data from representative mice are shown in Fig 6B. These data indicate that
358   increased licking was observed for higher concentrations of sucrose and that L-histidine
359   suppressed this licking. Analysis of grouped data by two-way ANOVA found a main effect of
360   injection (saline, mean 572.38 +/- SEM 64.22 vs. L-histidine, 244.88 +/- 58.09; $F_{1, 14}$ = 14.303 p =
361   0.002), such that mice with L-histidine injections licked less overall than mice with vehicle
362   injections. There was also a main effect of sucrose concentration ($F_{4, 56}$ = 172.432, p <0.001),
363   with mice licking more to higher concentrations of sucrose. The interaction between sucrose
364   concentration and injection type was also significant (Fig 6C; $F_{4, 56}$ = 11.182, p = 0.049). We
365   performed planned comparisons between injection types at each sucrose concentration, and
366   found that mice with L-histidine injections licked less than control mice at 0% (t_{14} = -3.882, p =
367   0.002), 5% (t_{14} = -2.258, p = 0.04), 10% (t_{14} = -2.243, p = 0.03), 20% (t_{14} = -4.293, p > 0.001), and
368   30% sucrose (t_{14} = -2.484, p = 0.026).

4. Discussion

370   Here, we show for the first time that a novel fluorescent histamine sensor, HisLightG, is
371   able to detect rapid fluctuations in histamine signaling while animals engage in ingestive
372   behavior. Although previous studies have used fiber photometry to measure histamine *in vivo*
373   (Dong et al., 2023; Lin et al., 2023), these studies use a different sensor (GRAB-HA). Availability
374   of multiple sensors for a single molecule is useful, as differences between sensor properties
375   (e.g., kinetics) can make a particular sensor more suitable for a given experiment; this has been
376   discussed in detail for dopamine sensors (Labouesse et al., 2020).

377   Our *in vitro* experiments clearly show that HisLightG responds to histamine. The
378   response to histamine compared to a variety of other neurotransmitters shows a high specificity
379   to histamine. Interestingly, acetylcholine elicited a small response, but this was an order of
380   magnitude smaller
381   than that of histamine, and indeed so small that it is extremely unlikely to cause any detectable
382   signals *in vivo*. In light of this, we have a high degree of confidence that our photometry
383   experiments were reliably measuring histamine release and not acetylcholine.

384   Past studies that have prevented histamine from exerting its normal function in particular

385   brain areas have identified the VMH and PVH as the regions responsible for histamine reducing

386   food intake (Ookuma et al., 1989, 1993; Sakata et al., 1988, 1990, 1991). Here, we examined

387   the dynamics of histamine in these areas during eating behavior and found both similarities and

388   differences in the histaminergic responses to consumption. In both regions, in food-restricted

389   mice, histamine decreased as licking commenced. It remained below baseline when licking

390   stopped. In the PVH, however, histamine rebounded to above baseline levels following the end

391   of licking, while in the VMH it remained suppressed. The functional implications of this difference

392   requires further investigation. A previous microdialysis experiment demonstrated a brief rise in

393   medial hypothalamic histamine after food deprived rats were given 15 min to eat (Itoh et al.,

394   1991). This increase in histamine was present on a timescale of minutes, indicating a modestly

395   prolonged response of histamine to food. We show that histamine is also altered on a timescale

396   of seconds during consumption of nutritive solutions when hungry, with changes closely linked to

397   individual lick bouts. Interestingly, the study by Itoh et al (1991) found an increase in medial

398   hypothalamus histamine after eating, while we found regional differences such that in the PVH

399   histamine increased after an eating bout, but the opposite was true in the VMH.

400   When we examined histamine release in each region during different conditions, we

401   again found some regional differences. In the PVH, histamine was suppressed during the lick

402   bout in all conditions. After the lick bout, histamine rebounded in the Restricted and Dark

403   Conditions. In the Light and Sucralose conditions, there was also a rebound but it was slower to

404   occur. This leaves open the possibility that hunger state and caloric content of the solution

405   influence the rebound of histamine in the PVH. Mice in the Restricted condition were hungry

406   because of the food restriction, and in the Dark condition were presumably hungry simply from it

407   being the time of day they normally eat. In the Light condition, the mice were likely less hungry

408   because during the light phase they are normally sleeping, not eating, and so when these mice

409   licked for Ensure, histamine release was different than when these same mice consumed

410   Ensure in a different hunger state. In the Sucralose condition, the mice were tested in the dark

411   phase and therefore equally hungry as when tested in the Dark phase, but the substance they

412   were given to lick contained no calories. Again, this appears to have influenced histamine

413   release in the PVH. In the VMH, in contrast, histamine remained suppressed from the start of

414   licking until at least 10 s after licking stopped in the Restricted, Dark, and Light conditions. In the

415   Sucralose condition, histamine showed no change from baseline during the first 2 s of licking,

416   but was then suppressed equally as in the other conditions.

417   Caloric content is one possible reason why histamine responses were different in the
418   Sucralose condition compared to the conditions in which mice were drinking Ensure, but it is
419   also plausible that the difference was instead taste-driven. Microdialysis experiments measuring
420   histamine in the anterior hypothalamus found that histamine levels respond to the nature of the
421   ingested substance. Specifically, perfusates from anterior hypothalamus of food deprived rats
422   receiving intraoral infusions of various tastants showed increased histamine after sodium
423   chloride, hydrochloric acid, and quinine, but a decreased histamine response after saccharin or
424   sucrose (Treesukosol et al., 2005). Interestingly, when saccharin or sucrose was paired with
425   lithium chloride to produce a conditioned taste aversion, these tastes produced an increase in
426   histamine (Treesukosol et al., 2005). The authors conclude that histamine release may reflect
427   palatability of the ingested substance, with decreases indicative of high palatability. Both of our
428   test solutions – "Ensure" and sucralose – are generally considered palatable, and this is
429   consistent with the reduced histamine seen during licking. Whether this is related to the
430   sustained histamine sumpression in the VMH after licking stops, and why the same solutions
431   caused an increase after licking in the PVH, requires further study.

432   A fall in VMH histamine could reflect the palatability of the solution, but it is also likely that
433   it is related to the role of histamine in suppressing food intake. Higher levels of histamine are
434   associated with decreased food intake, so the reduction in histamine during eating could be
435   promoting continued consumption, both within that lick bout and increasing the likelihood of
436   subsequent lick bouts occurring due to the continued suppression. The fact that histamine in the
437   PVH returns to baseline after a lick bout – rather than remaining suppressed as in the VMH –
438   could mean that these regions have distinct roles in appetite regulation.

439   To demonstrate a role for increased histamine levels in suppressing feeding, we
440   performed a test in a recently developed multispout apparatus (Gordon-Fennell et al., 2023) in
441   which it was possible to test licking across several different concentrations of sucrose. In this
442   test we found that increasing histamine levels by injecting the histamine precursor, L-histidine,
443   suppressed licking. Thus, this links increased histamine to reduced licking and potentially satiety
444   mechanisms. Future experiments using this method can determine whether antagonizing
445   specific histamine receptors in specific brain regions is able to block this suppressive effect of L-
446   histidine on licking behavior.

447   In summary, here we show that the fluorescent histamine sensor, HisLightG, can be used
448   to detect rapid fluctuations in histamine release associated with eating bouts and that these
449   patterns of release show some regional heterogeneity and sensitivity to the caloric content of the
450   ingested substance.

451

452

453 **Conflict of interest statement**: The authors declare no competing financial interests.

454

461

462 **Author contributions:** Designed research, KLV, GDS, TP, AGG-F, JEM; Performed
463 research, KLV, AG, BB, HT, MV, AGG-F, JEM; Analyzed data, KLV, AG, JEM; Wrote the paper,
464 KLV, JEM.

465

References

Attoub, S., Moizo, L., Sobhani, I., Laigneau, J.-P., Lewin, M. J. M., & Bado, A. (2001). The H3 receptor is involved in cholecystokinin inhibition of food intake in rats. *Life Sciences*, *69*(4), 469–478. https://doi.org/10.1016/S0024-3205(01)01138-9

Berger, S. N., Baumberger, B., Samaranayake, S., Hersey, M., Mena, S., Bain, I., Duncan, W., Reed, M. C., Nijhout, H. F., Best, J., & Hashemi, P. (2022). An In Vivo Definition of Brain Histamine Dynamics Reveals Critical Neuromodulatory Roles for This Elusive Messenger. *International Journal of Molecular Sciences*, *23*(23). https://doi.org/10.3390/ijms232314862

D'Este, L., Wimalawansa, S. J., & Renda, T. G. (2001). Distribution of Amylin-Immunoreactive Neurons in the Monkey Hypothalamus and their Relationships with the Histaminergic System. *Archives of Histology and Cytology*, *64*(3), 295–303. https://doi.org/10.1679/aohc.64.295

Doi, T., Sakata, T., Yoshimatsu, H., Machidori, H., Kurokawa, M., Jayasekara, L. A. L. W., & Niki, N. (1994). Hypothalamic neuronal histamine regulates feeding circadian rhythm in rats. *Brain Research*, *641*(2), 311–318. https://doi.org/10.1016/0006-8993(94)90160-0

Dong, H., Li, M., Yan, Y., Qian, T., Lin, Y., Ma, X., Vischer, H. F., Liu, C., Li, G., Wang, H., Leurs, R., & Li, Y. (2023). Genetically encoded sensors for measuring histamine release both in vitro and in vivo. *Neuron*, *111*(10), 1564-1576.e6. https://doi.org/10.1016/j.neuron.2023.02.024

Fukagawa, K., Sakata, T., Shiraishi, T., Yoshimatsu, H., Fujimoto, K., Ookuma, K., & Wada, H. (1989). Neuronal histamine modulates feeding behavior through H1-receptor in rat hypothalamus. *American Journal of Physiology-Regulatory, Integrative and Comparative Physiology*, *256*(3), R605–R611. https://doi.org/10.1152/ajpregu.1989.256.3.R605

Futagawa, A., Tsuneoka, Y., Lazarus, M., & Oishi, Y. (2024). Comprehensive mapping of histamine H$_1$ receptor mRNA in the mouse brain. *Journal of Comparative Neurology*, *532*(5), e25622. https://doi.org/10.1002/cne.25622

Gordon-Fennell, A., Barbakh, J. M., Utley, M. T., Singh, S., Bazzino, P., Gowrishankar, R., Bruchas, M. R., Roitman, M. F., & Stuber, G. D. (2023). An open-source platform for head-fixed operant and consummatory behavior. *eLife*, *12*, e86183. https://doi.org/10.7554/eLife.86183

Gotoh, K., Fukagawa, K., Fukagawa, T., Noguchi, H., Kakuma, T., Sakata, T., & Yoshimatsu, H. (2005). Glucagon-like peptide-1, corticotropin-releasing hormone, and hypothalamic neuronal histamine interact in the leptin-signaling pathway to regulate feeding behavior. *The FASEB Journal*, *19*(9), 1131–1133. https://doi.org/10.1096/fj.04-2384fje

Itoh, Y., Oishi, R., & Saeki, K. (1991). Feeding-induced increase in the extracellular concentration of histamine in rat hypothalamus as measured by in vivo microdialysis. *Neuroscience Letters*, *125*(2), 235–237. https://doi.org/10.1016/0304-3940(91)90037-T

503 Jean-Richard-dit-Bressel, P., Clifford, C. W. G., & McNally, G. P. (2020). Analyzing Event-Related
504   Transients: Confidence Intervals, Permutation Tests, and Consecutive Thresholds.
505   *Frontiers in Molecular Neuroscience*, *13*, 14. https://doi.org/10.3389/fnmol.2020.00014

506 Kagiampaki, Z., Rohner, V., Kiss, C., Curreli, S., Dieter, A., Wilhelm, M., Harada, M., Duss, S. N.,
507   Dernic, J., Bhat, M. A., Zhou, X., Ravotto, L., Ziebarth, T., Wasielewski, L. M., Sönmez,
508   L., Benke, D., Weber, B., Bohacek, J., Reiner, A., … Patriarchi, T. (2023). Sensitive
509   multicolor indicators for monitoring norepinephrine in vivo. *Nature Methods*, *20*(9), 1426–
510   1436. https://doi.org/10.1038/s41592-023-01959-z

511 Konanur, V. R., Hsu, T. M., Kanoski, S. E., Hayes, M. R., & Roitman, M. F. (2020). Phasic
512   dopamine responses to a food-predictive cue are suppressed by the glucagon-like
513   peptide-1 receptor agonist Exendin-4. *Physiology & Behavior*, *215*, 112771.
514   https://doi.org/10.1016/j.physbeh.2019.112771

515 Kurose, Y., & Terashima, Y. (1999). Histamine regulates food intake through modulating
516   noradrenaline release in the para-ventricular nucleus. *Brain Research*, *828*(1–2), 115–
517   118. https://doi.org/10.1016/S0006-8993(99)01339-6

518 Labouesse, M. A., Cola, R. B., & Patriarchi, T. (2020). GPCR-Based Dopamine Sensors—A
519   Detailed Guide to Inform Sensor Choice for In Vivo Imaging. *International Journal of
520   Molecular Sciences*, *21*(21), 8048. https://doi.org/10.3390/ijms21218048

521 Lecklin, A., Etu-Seppälä, P., Stark, H., & Tuomisto, L. (1998). Effects of intracerebroventricularly
522   infused histamine and selective H1, H2 and H3 agonists on food and water intake and
523   urine flow in Wistar rats. *Brain Research*, *793*(1–2), 279–288.
524   https://doi.org/10.1016/S0006-8993(98)00186-3

525 Lin, W., Xu, L., Zheng, Y., An, S., Zhao, M., Hu, W., Li, M., Dong, H., Li, A., Li, Y., Gong, H., Pan,
526   G., Wang, Y., Luo, Q., & Chen, Z. (2023). Whole-brain mapping of histaminergic
527   projections in mouse brain. *Proceedings of the National Academy of Sciences*, *120*(14),
528   13–25. https://doi.org/10.1073/pnas.2216231120

529 Lutz, T. A., Del Prete, E., Walzer, B., & Scharrer, E. (1996). The histaminergic, but not the
530   serotoninergic, system mediates amylin's anorectic effect. *Peptides*, *17*(8), 1317–1322.
531   https://doi.org/10.1016/S0196-9781(96)00199-4

532 Masaki, T., Chiba, S., Yasuda, T., Noguchi, H., Kakuma, T., Watanabe, T., Sakata, T., &
533   Yoshimatsu, H. (2004). Involvement of hypothalamic histamine H1 receptor in the
534   regulation of feeding rhythm and obesity. *Diabetes*, *53*(9), 2250–2260.
535   https://doi.org/10.2337/diabetes.53.9.2250

536 Michael, N. J., Caron, A., Lee, C. E., Castorena, C. M., Lee, S., Zigman, J. M., Williams, K. W., &
537   Elmquist, J. K. (2020). Melanocortin regulation of histaminergic neurons via perifornical
538   lateral hypothalamic melanocortin 4 receptors. *Molecular Metabolism*, *35*, 100956.
539   https://doi.org/10.1016/j.molmet.2020.01.020

540 Mirdita, M., Schütze, K., Moriwaki, Y., Heo, L., Ovchinnikov, S., & Steinegger, M. (2022).
541   ColabFold: Making protein folding accessible to all. *Nature Methods*, *19*(6), 679–682.
542   https://doi.org/10.1038/s41592-022-01488-1

Mochizuki, T., Yamatodani, A., Okakura, K., Horii, A., Inagaki, N., & Wada, H. (1992). Circadian rhythm of histamine release from the hypothalamus of freely moving rats. *Physiology and Behavior*, *51*(2), 391–394. https://doi.org/10.1016/0031-9384(92)90157-W

Mollet, A., Meier, S., Riediger, T., & Lutz, T. A. (2003). Histamine H1 receptors in the ventromedial hypothalamus mediate the anorectic action of the pancreatic hormone amylin. *Peptides*, *24*(1), 155–158. https://doi.org/10.1016/S0196-9781(02)00288-7

Morimoto, T., Yamamoto, Y., Mobarakeh, J. I., Yanai, K., Watanabe, T., Watanabe, T., & Yamatodani, A. (1999). Involvement of the histaminergic system in leptin-induced suppression of food intake. *Physiology and Behavior*, *67*(5), 679–683. https://doi.org/10.1016/S0031-9384(99)00123-7

Ookuma, K., Sakata, T., Fukagawa, K., Yoshimatsu, H., Kurokawa, M., Machidori, H., & Fujimoto, K. (1993). Neuronal histamine in the hypothalamus suppresses food intake in rats. *Brain Research*, *628*(1–2), 235–242. https://doi.org/10.1016/0006-8993(93)90960-U

Ookuma, K., Yoshimatsu, H., Sakata, T., Fujimoto, K., & Fukagawa, K. (1989). Hypothalamic sites of neuronal histamine action on food intake by rats. *Brain Research*, *490*(2), 268–275. https://doi.org/10.1016/0006-8993(89)90244-8

Panula, P., Pirvola, U., Auvinen, S., & Airaksinen, M. S. (1989). Histamine-immunoreactive nerve fibers in the rat brain. *Neuroscience*, *28*(3), 585–610. https://doi.org/10.1016/0306-4522(89)90007-9

Panula, P., Yang, H. Y. T., & Costa, E. (1984). Histamine-containing neurons in the rat hypothalamus. *Proceedings of the National Academy of Sciences of the United States of America*, *81*(8 I), 2572–2576. https://doi.org/10.1073/pnas.81.8.2572

Patriarchi, T., Cho, J. R., Merten, K., Marley, A., Broussard, G. J., Liang, R., Williams, J., Nimmerjahn, A., Von Zastrow, M., Gradinaru, V., & Tian, L. (2019). Imaging neuromodulators with high spatiotemporal resolution using genetically encoded indicators. *Nature Protocols*, *14*(12), 3471–3505. https://doi.org/10.1038/s41596-019-0239-2

Sakata, T., Fukagawa, K., Fujimoto, K., Yoshimatsu, H., Shiraishi, T., & Wada, H. (1988). Feeding induced by blockade of histamine H1-receptor in rat brain. *Experientia*, *44*(3), 216–218. https://doi.org/10.1007/BF01941710

Sakata, T., Fukagawa, K., Ookuma, K., Fujimoto, K., Yoshimatsu, H., Yamatodani, A., & Wada, H. (1990). Hypothalamic neuronal histamine modulates ad libitum feeding by rats. *Brain Research*, *537*(1–2), 303–306. https://doi.org/10.1016/0006-8993(90)90373-J

Sakata, T., Kurokawa, M., Oohara, A., & Yoshimatsu, H. (1994). A physiological role of brain histamine during energy deficiency. *Brain Research Bulletin*, *35*(2), 135–139. https://doi.org/10.1016/0361-9230(94)90093-0

Sakata, T., Ookuma, K., Fujimoto, K., Fukagawa, K., & Hironobu, Y. (1991). Histaminergic control of energy balance in rats. *Brain Research Bulletin*, *27*(3–4), 371–375. https://doi.org/10.1016/0361-9230(91)90127-6

582   Samaranayake, S., Abdalla, A., Robke, R., Wood, K. M., Zeqja, A., & Hashemi, P. (2015). In vivo
583   histamine voltammetry in the mouse premammillary nucleus. *Analyst*, *140*(11), 3759–
584   3765. https://doi.org/10.1039/c5an00313j

585   Simpson, E. H., Akam, T., Patriarchi, T., Blanco-Pozo, M., Burgeno, L. M., Mohebi, A., Cragg, S.
586   J., & Walton, M. E. (2024). Lights, fiber, action! A primer on in vivo fiber photometry.
587   *Neuron*, *112*(5), 718–739. https://doi.org/10.1016/j.neuron.2023.11.016

588   Toftegaard, C. L., Knigge, U., Kjær, A., & Warberg, J. (2003). The role of hypothalamic histamine
589   in leptin-induced suppression of short-term food intake in fasted rats. *Regulatory*
590   *Peptides*, *111*(1–3), 83–90. https://doi.org/10.1016/S0167-0115(02)00260-4

591   Treesukosol, Y., Ishizuka, T., Yamamoto, C., Senda, K., Tsutsumi, S., Yamatodani, A., &
592   Yamamoto, T. (2005). Hypothalamic histamine release by taste stimuli in freely moving
593   rats: Possible implication of palatability. *Behavioural Brain Research*, *164*(1), 67–72.
594   https://doi.org/10.1016/j.bbr.2005.06.004

595   Watanabe, T., Taguchi, Y., Shiosaka, S., Tanaka, J., Kubota, H., Terano, Y., Tohyama, M., &
596   Wada, H. (1984). Distribution of the histaminergic neuron system in the central nervous
597   system of rats; a fluorescent immunohistochemical analysis with histidine decarboxylase
598   as a marker. *Brain Research*, *295*(1), 13–25. https://doi.org/10.1016/0006-
599   8993(84)90811-4

600

601

Table caption

Table 1. Surgical coordinates. Coordinates used to target the PVH and VMH are provided, including the medial-lateral, anterior-posterior, and dorsal-ventral coordinates relative to bregma and based on a flat skull.

Table 2: Number of lick bouts contributing to the photometry analysis. Number of lick bouts >4 s that were used to analyze changes in histamine during different conditions. Total lick bouts included, as well as number from each of the mice, are displayed.

Figure captions

Figure 1. *In vitro* results. (A) Structural model of HisLightG (Kagiampaki et al., 2023) obtained through AlphaFold2 (Mirdita et al., 2022). Indicated in green are the grafted components from dLight1.3b, and in tan the original sequence from the human H4 histamine receptor. (B) Representative images of HisLightG-expressing HEK293T cells in the presence or absence of Histamine (10 µM) and corresponding signal-to-noise (SNR) heatmap. (C) Quantification of the fluorescence response of HisLightG to different non-ligand neurotransmitters (10 µM) in HEK293T cells. Data are shown as response of individual cells, with vertical lines indicating the mean for that neurotransmitter. * $p < 0.05$ relative to HBSS.

Figure 2. Schematic and licking behavior. A timeline of the experiment shows the number and order of photometry sessions; mice in both the PVH and VMH cohorts were tested in the same conditions and order of conditions (A). The total number of lick bouts (i.e. those that contained at least 3 licks and which were separated from another licking bout by at least 10 seconds) across all mice and sessions for each condition, plotted against bout length, is displayed (B). Lick frequency was similar in all conditions except Sucralose (C). Condition affected how much mice licked on average in each session (D). Condition also influenced the number of bouts per session (E). The average length of bouts, in seconds, also differed by Condition (F). Bars are means and circles individual data points, lower-case letters indicate $p < 0.05$ (e.g., a is different from b).

Figure 3. Histology and representative photometry responses in PVH and VMH. Illustration of viral spread and fiber tip location in mice included in the PVH analysis (A) and VMH analysis (B) with approximate bregma indicated. The green color shows the presence of HislightG and the grey color the fiber tip; each animal (n=7 per region) is represented by a semi-transparent shape. Images of representative animals with PVH (C) and VMH (D) injections are also shown. A

22

634   heatmap showing the z-scored change in fluorescence before, during, and after a lick bout for all

635   valid lick bouts (n=39) in a representative mouse with HisLightG in the PVH, as well as the trace

636   of the average of those trials (E). The individual lick bouts (n=31) and the average of those for a
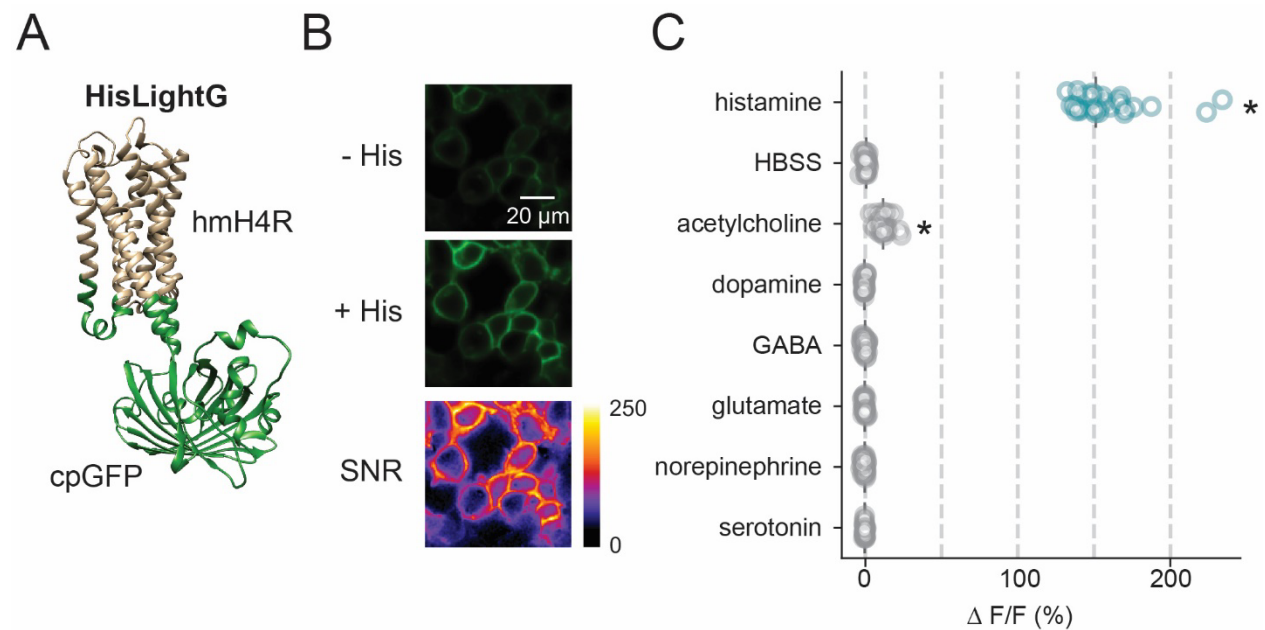
637   mouse with HisLightG in the VMH (F).

638   **Figure 4. Histamine in the PVH and VMH during consumption of "Ensure" while food**

639   **restricted.** Each lick bout that met the criteria for photometry analysis was plotted in a heatmap,

640   sorted based on post-licking z-score. This reveals an apparent difference between the PVH and

641   the VMH (A). The difference in histamine was confirmed by waveform analysis, which showed

642   that these regions differed from each other from the last 2 s of licking until at least 10 s after

643   licking stopped; in the VMH histamine remained below baseline from the beginning of the lick

644   bout until the end of the 10 s post-lick period, whereas in the PVH histamine was reduced during

645   licking and for the first seconds after licking stopped, at which point it rebounded to above

646   baseline levels (B).

647   **Figure 5. Histamine release across different conditions.** In the PVH (A), histamine traces

648   show no major differences between Dark and Restricted conditions, but a slower rebound in the

649   post-lick period in the Light and Sucralose. In the VMH (B), there were no differences in

650   histamine in the Restricted, Dark, and Light conditions, but no reduction in histamine during early

651   licking in the Sucralose condition.

652   **Figure 6. Increasing histamine suppresses sucrose intake.** Mice were trained to lick in an

653   OHRBETS multispout apparatus (A). Raster plots from representative mice show less licking in

654   the mouse given a systemic injection of the histamine precursor, L-histidine (B), and this was

655   also evident in the grouped data where total licks were reduced when mice were given L-

656   histidine. Main effects of both sucrose concentration and drug administration were observed with

657   planned comparisons showing that licks per trial were lower to at all sucrose concentrations

658   when mice were administered L-histidine (C). Bars are means and circles individual data points.
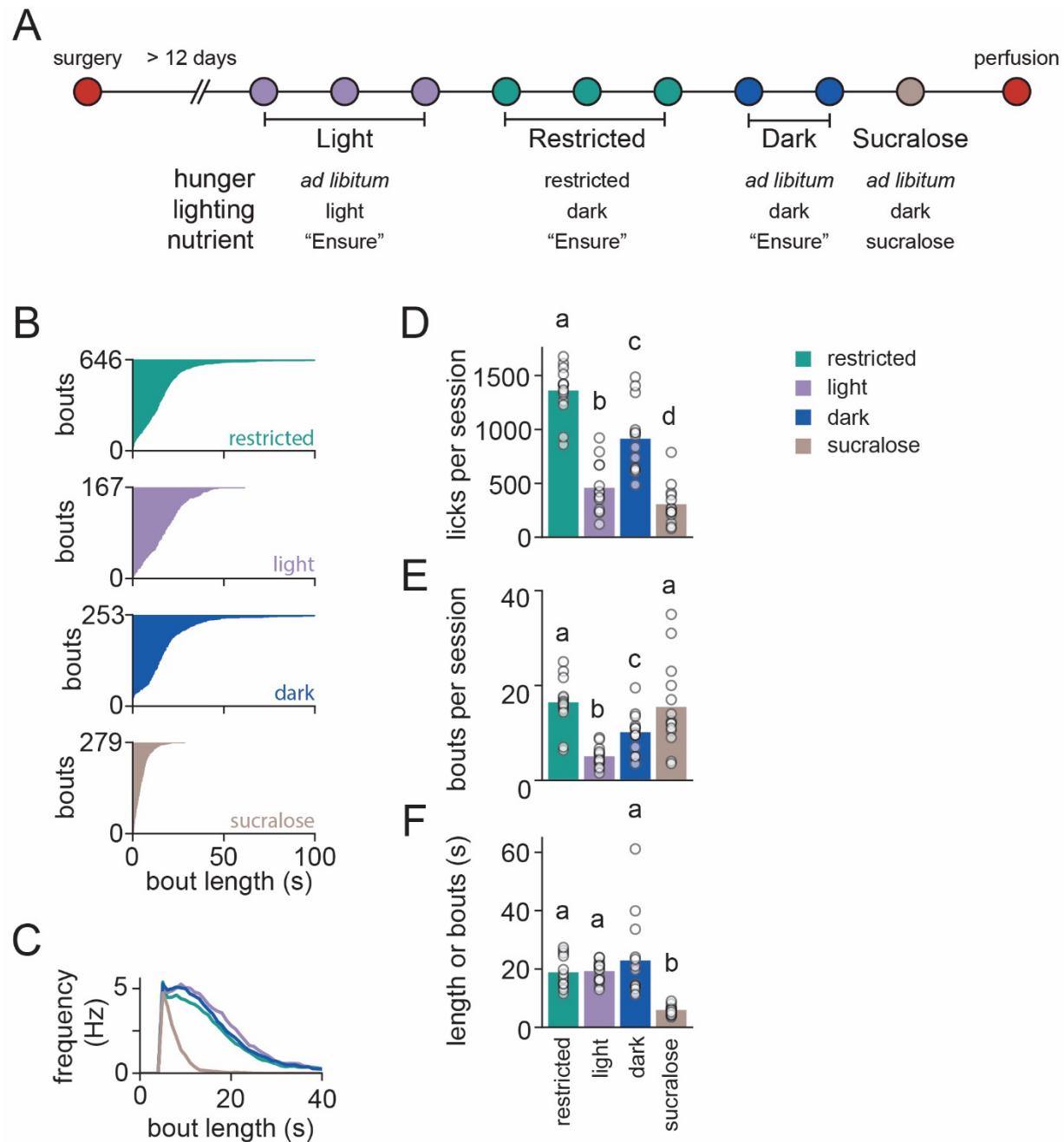
659    $* p < 0.05$

660

661 **Figure Supplemental 1. Area Under the Curve analysis of histamine in the PVH and VMH**

662 **of mice drinking Ensure while food restricted.** Each subject's average Z-score across all lick

663 bouts and sessions for mice with HisLightG in the PVH and VMH shows inter-subject

664 consistency (A), and plotting the average for each region shows a stark difference in histamine

665 release between regions (B). We averaged the data from all trials for each mouse (n=7 for each

666 region) and compared changes in the AUC between regions and across time; time was divided

667 into 5 epochs: baseline, the first 6 s of a lick bout (early licking), the last 2 s of a lick bout (late

668 licking), the 5 s immediately after licking (early post), and the 5 s following that (late post). We

669 found significant main effects of Time ($F_{4, 48}$ = 21.047, p = <0.001) and Region ($F_{1, 12}$ = 18.944, p

670 = <0.001), as well as a significant interaction between the two ($F_{4, 48}$ = 18.518, p = <0.001).

671 Holm-corrected post hoc tests revealed that in the PVH, only the late licking epoch had a lower

672 AUC than the baseline epoch, while in the VMH, the late licking, early post, and late post epochs

673 all had lower AUCs than baseline. Furthermore, in both post-licking epochs, the AUC of PVH and

674 VMH differed from one another (C). Bars are means and circles individual data points, # p <

675 0.05 from baseline for that region, * p < 0.05 between regions for that epoch.
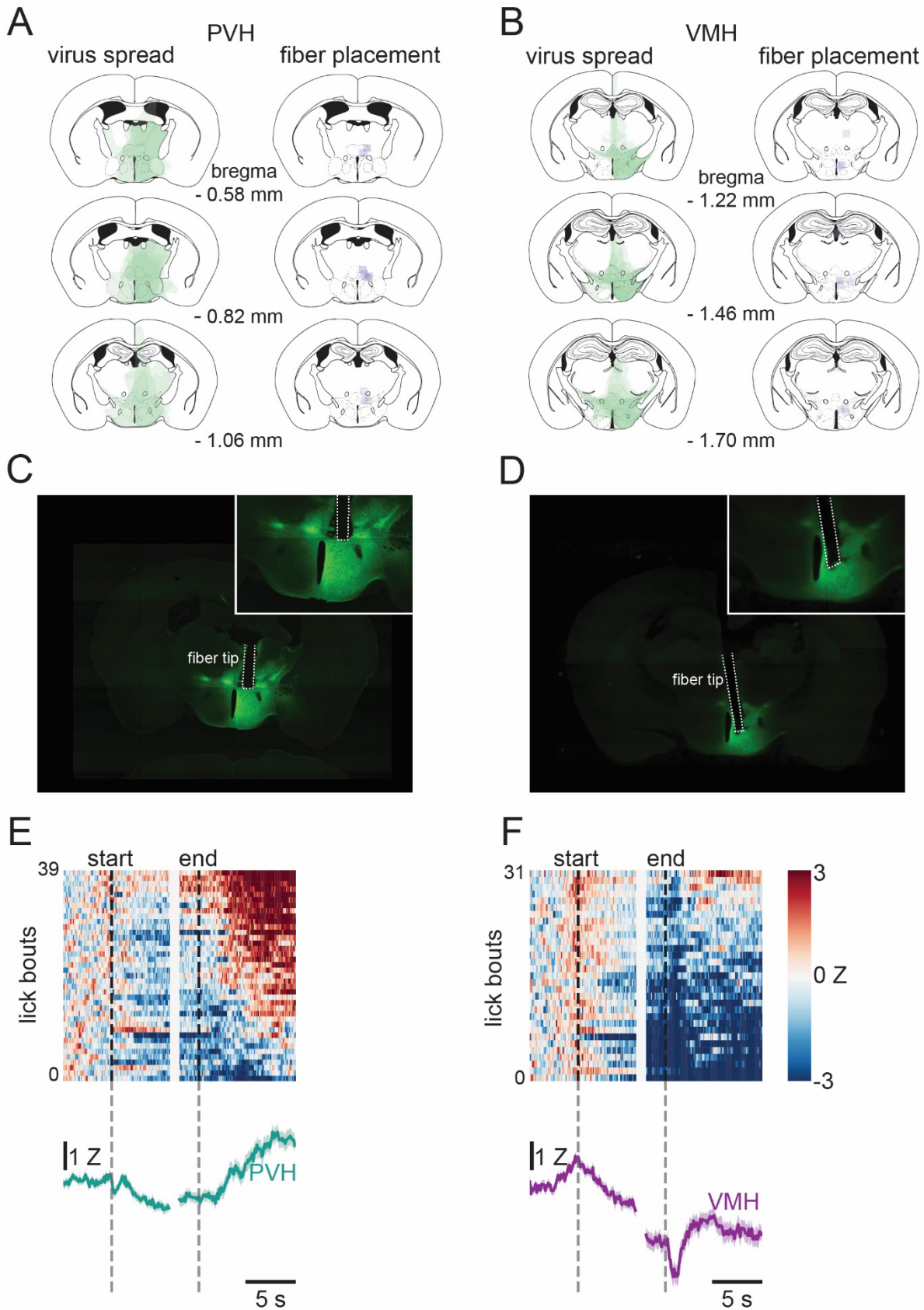
676

Figure 1. *In vitro* results. (A) Structural model of HisLightG (Kagiampaki et al., 2023) obtained through AlphaFold2 (Mirdita et al., 2022). Indicated in green are the grafted components from dLight1.3b, and in tan the original sequence from the human H4 histamine receptor. (B) Representative images of HisLightG-expressing HEK293T cells in the presence or absence of Histamine (10 µM) and corresponding signal-to-noise (SNR) heatmap. (C) Quantification of the fluorescence response of HisLightG to different non-ligand neurotransmitters (10 µM) in HEK293T cells. Data are shown as response of individual cells, with vertical lines indicating the mean for that neurotransmitter. * $p < 0.05$ relative to HBSS.

677

Figure 2. Schematic and licking behavior. A timeline of the experiment shows the number and order of photometry sessions; mice in both the PVH and VMH cohorts were tested in the same conditions and order of conditions (A). The total number of lick bouts (i.e. those that contained at least 3 licks and which were separated from another licking bout by at least 10 seconds) across all mice and sessions for each condition, plotted against bout length, is displayed (B). Lick frequency was similar in all conditions except Sucralose (C). Condition affected how much mice licked on average in each session (D). Condition also influenced the number of bouts per session (E). The average length of bouts, in seconds, also differed by Condition (F). Bars are means and circles individual data points, lower-case letters indicate p < 0.05 (e.g., a is different from b).

678

679

Figure 3. Histology and representative photometry responses in PVH and VMH. Illustration of viral spread and fiber tip location in mice included in the PVH analysis (A) and VMH analysis (B) with approximate bregma indicated. The green color shows the presence of HislightG and the grey color the fiber tip; each animal (n=7 per region) is represented by a semi-transparent shape. Images of representative animals with PVH (C) and VMH (D) injections are also shown. A heatmap showing the z-scored change in fluorescence before, during, and after a lick bout for all valid lick bouts (n=39) in a representative mouse with HisLightG in the PVH, as well as the trace of the average of those trials (E). The individual lick bouts (n=31) and the average of those for a mouse with HisLightG in the VMH (F).

680
681

682
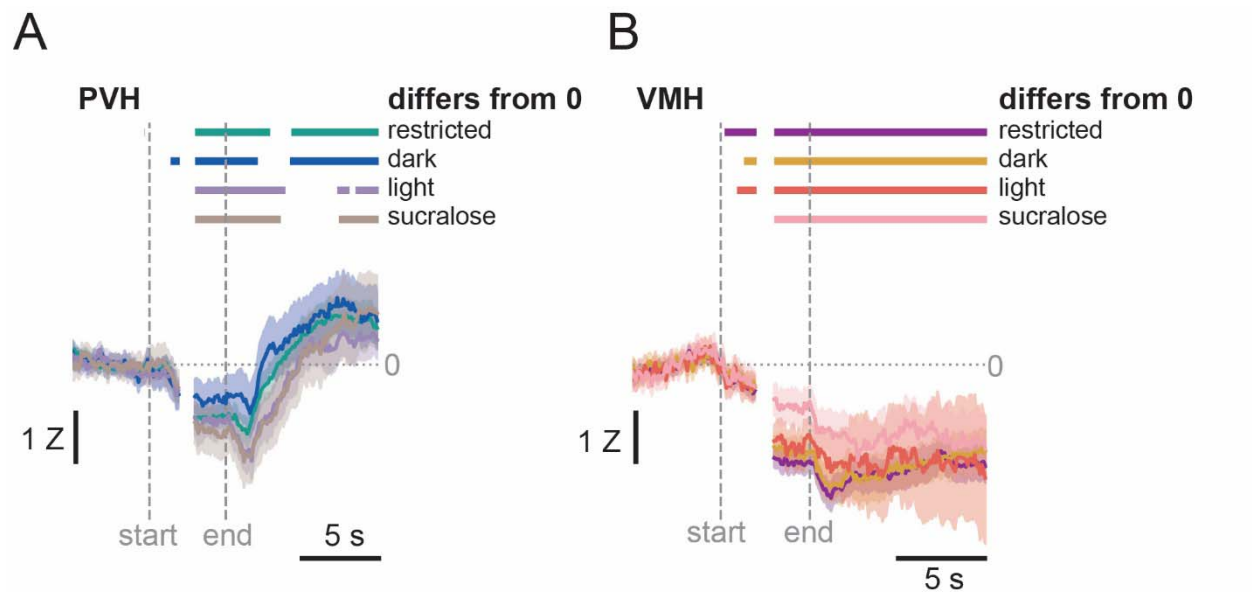
Figure 5. Histamine release across different conditions. In the PVH (A), histamine traces show no major differences between Dark and Restricted conditions, but a slower rebound in the post-lick period in the Light and Sucralose. In the VMH (B), there were no differences in histamine in the Restricted, Dark, and Light conditions, but no reduction in histamine during early licking in the Sucralose condition.
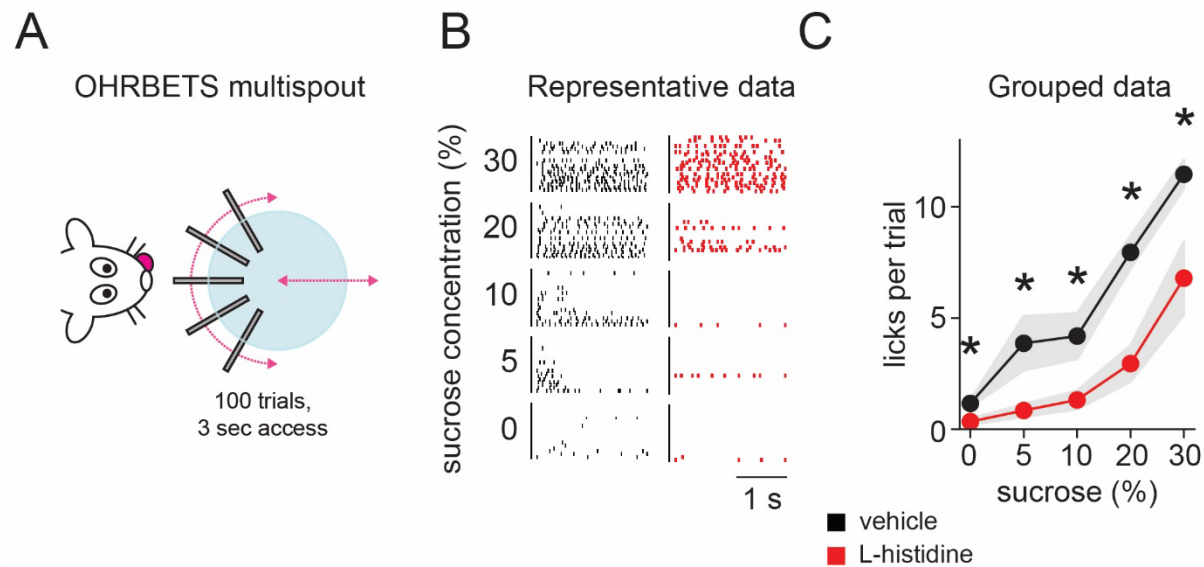
Figure 6. Increasing histamine suppresses sucrose intake. Mice were trained to lick in an OHRBETS multispout apparatus (A). Raster plots from representative mice show less licking in the mouse given a systemic injection of the histamine precursor, L-histidine (B), and this was also evident in the grouped data where total licks were reduced when mice were given L-histidine. Main effects of both sucrose concentration and drug administration were observed with planned comparisons showing that licks per trial were lower to at all sucrose concentrations when mice were administered L-histidine (C). Bars are means and circles individual data points. * p < 0.05
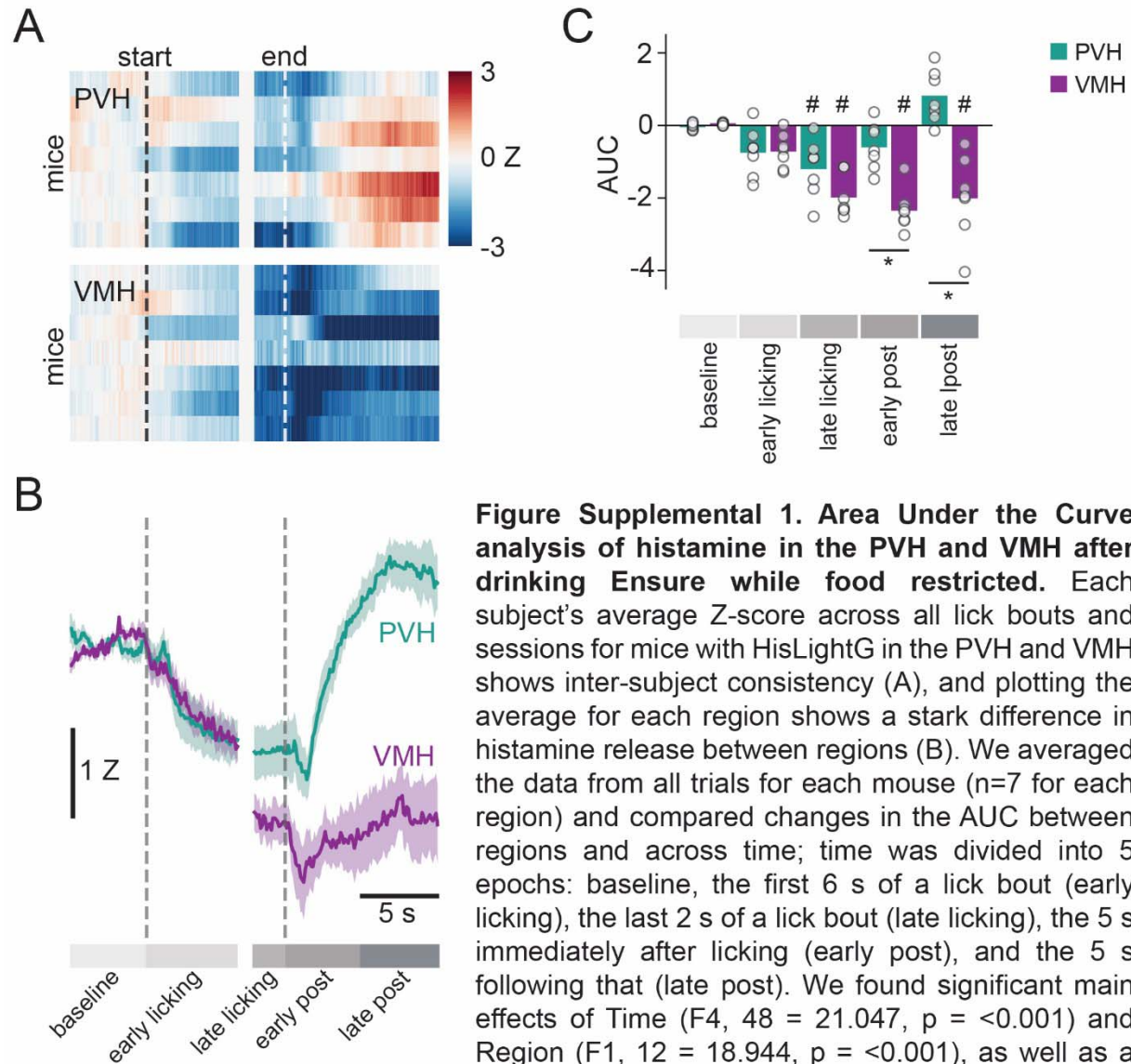
Figure Supplemental 1. Area Under the Curve analysis of histamine in the PVH and VMH after drinking Ensure while food restricted. Each subject's average Z-score across all lick bouts and sessions for mice with HisLightG in the PVH and VMH shows inter-subject consistency (A), and plotting the average for each region shows a stark difference in histamine release between regions (B). We averaged the data from all trials for each mouse (n=7 for each region) and compared changes in the AUC between regions and across time; time was divided into 5 epochs: baseline, the first 6 s of a lick bout (early licking), the last 2 s of a lick bout (late licking), the 5 s immediately after licking (early post), and the 5 s following that (late post). We found significant main effects of Time ($F_{4, 48} = 21.047$, $p = <0.001$) and Region ($F_{1, 12} = 18.944$, $p = <0.001$), as well as a significant interaction between the two ($F_{4, 48} = 18.518$, $p = <0.001$). Holm-corrected post hoc tests revealed that in the PVH, only the late licking epoch had a lower AUC than the baseline epoch, while in the VMH, the late licking, early post, and late post epochs all had lower AUCs than baseline. Furthermore, in both post-licking epochs, the AUC of PVH and VMH differed from one another (C). Bars are means and circles individual data points, # $p < 0.05$ from baseline for that region, * $p < 0.05$ between regions for that epoch.

32